

Moldability and Solvent Debinding of Hydroxyapatite Micro-Part Processed through Micro-Powder Injection Molding

Al Basir*, Norhamidi Muhamad, Abu Bakar Sulong, Mohammad Fadhli Izuddin Bin Mohd Nor,
 Muhammad bin Mohamed Amin & Nashrah Hani Jamadon

*Department of Mechanical and Manufacturing Engineering, Faculty of Engineering and Built Environment,
 Universiti Kebangsaan Malaysia, 43600 Bangi, Selangor, Malaysia*

*Corresponding author: al.basir005@yahoo.com

Received 17 April 2023, Received in revised form 6 August 2023
 Accepted 30 October 2023, Available online 30 March 2024

ABSTRACT

The development of the micro-powder injection molding (μ PIM) process from the powder injection molding (PIM) process has been prompted by the demand of the worldwide market to produce micro-sized components. The need for μ PIM-processed components is currently rising across a range of industries, including automotive, aerospace, food, biomedical, electronics, and telecommunications. In the current research work, homogeneous HA feedstock with a powder loading of 57 vol.% was prepared by mixing HA powder particles with palm stearin and low-density polyethylene (LDPE) binders at a mixing temperature of 150 °C for 6 h. Defect-free injection molded or green micro-sized components of HA were produced by employing injection pressure, injection time, mold temperature, and melt temperature of 12 bar, 5 s, 110 °C, and 180 °C, respectively. When mold temperatures less than 110 °C were used, short shot defects were frequently observed in green specimens. After solvent debinding at 60 °C for 50 min, 82.2% of the palm stearin was removed from the green part. No difference in dimension between the solvent debound part and the green part was noticed. An open-pore structure developed in the solvent debound HA micro-component is helpful for eliminating the insoluble LDPE binder during the thermal debinding phase.

Keywords: Micro-powder injection molding; Hydroxyapatite; Feedstock; Solvent debinding

INTRODUCTION

Powder injection molding (PIM) is a popular fabrication technology and a cost-effective way for generating complex, near net form macro-parts in powder metallurgy (Aslam et al. 2016; Basir et al. 2023; Basir et al. 2021a; Crozier-Bioud et al. 2023; Li et al. 2022; Liu et al. 2023a; Shu et al. 2022; Tafti et al. 2023). PIM technology is used in a variety of industries, including electronics, biomedical, aerospace, defense, and automotive engineering (Basir et al. 2021b; Dehghan-Manshadi et al. 2018; Liu et al. 2023b; Martinková et al. 2022). PIM has a number of benefits, such as numerous material alternatives, little waste, and great performance (Aslam et al. 2016, Dehghan-Manshadi et al. 2018, Liu et al. 2023a). The current preference of global market for the production of micro-parts for using in various technical applications has sped up the

development of micro-powder injection molding (μ PIM) from PIM (Attia et al. 2014; Basir et al. 2022a; Basir et al. 2022b; Liu et al. 2018; Wang et al. 2014). The μ PIM method is used to produce micro-parts, which have an extrinsic dimension of only a few millimeters, as opposed to the macro-parts, which have an average size of close to a few centimeters (Meng et al. 2011). Similar to PIM, using the μ PIM technique makes it feasible to fabricate metal and ceramic-based micro-parts in an economical manner. In recent years, the electronics, biomedical, and automotive industries have seen an increase in demand for μ PIM-processed micro-parts due to their high performance and cost-effectiveness (Attia et al. 2014; Bitar et al. 2012; Fayyaz et al. 2014; Foudzi et al. 2013; Piotter et al. 2011; Fu et al. 2004). Mixing, injection molding, debinding, and sintering are the four fundamental steps in the fabrication of micro components using μ PIM. A homogenized feedstock is produced through the mix of a fine powder

with an organic binder. The next step is to inject the feedstock into a small cavity of mold to generate the green micro-part, which takes on the appropriate shape. Using the proper method, the debinding procedure removes the binder from the molded part. In order to produce high density components along with desired mechanical properties, the debound micro-sized component is finally sintered (Attia & Alcock 2012; Foudzi et al. 2013; Jung et al. 2015; Meng et al. 2010; Park et al. 2018; Tay et al. 2009; Wang et al. 2022).

Modern materials science and engineering are facing significant challenges with the development of sophisticated materials for biomedical applications, particularly when it comes to the development of materials that can be employed *in vivo*. Due to its ability to form a strong, reliable association with bone tissue, hydroxyapatite (HA) has shown to be the best bone substitute. Additionally, it can exhibit osteoconductive behavior and has no negative impacts on human body (Aziz et al. 2015; Arifin et al. 2014; Alshammari et al. 2023; Hussin et al. 2022; Orlovskii et al. 2002; Siddiqui et al. 2018, Tan et al. 2013). Overall, HA is renowned for its exceptional biocompatibility and

corrosion resistance. Micro-sized HA components are increasingly in demand on the global market for usage in various biomedical applications. Therefore, in this study, the moldability and solvent debinding behavior of HA micro-sized components fabricated through the μ PIM technique was investigated.

EXPERIMENTAL PROCEDURES

In this study, the raw material used was HA powder from Vistec Technology Services, Malaysia, with mean particle size of $1.7 \mu\text{m}$. The pycnometer density of HA was 2.4831 g/cm^3 . The field emission scanning electron microscope (FESEM, Zeiss Merlin Compact) was used to inspect the morphology of HA powder and is displayed in Figure 1. In this investigation, the binder system was made up of 60 wt.% of palm stearin and 40 wt.% of low-density polyethylene (LDPE). Palm stearin and LDPE, which were supplied by Sime Darby Kempas Sdn. Bhd. and Polyolefin Company (Singapore) Pte Ltd., respectively, had densities of 0.891 and 0.91 g/cm^3 , respectively.

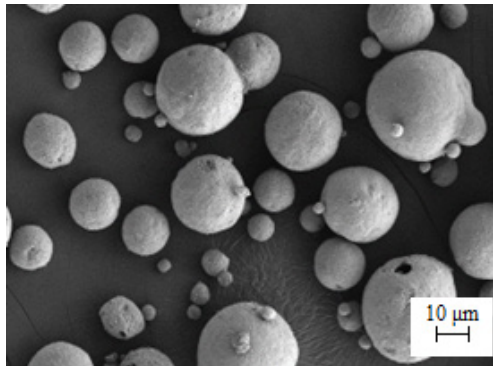


FIGURE 1. Morphology of HA powder

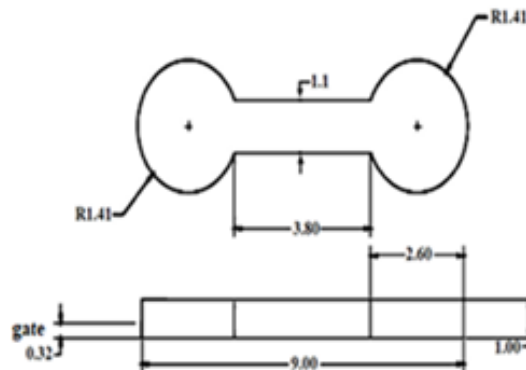


FIGURE 2. Schematic of HA micro-part (All the dimensions are in mm)

A W50 EHT Brabender mixer was used to fabricate the HA feedstock, with 57 vol.% of the HA being mixed with palm stearin and LDPE binders while upholding the temperature of mixing, time, and rotational speed of 150 °C, 6 h, and 25 rpm, respectively. Using the proper injection molding parameters, HA micro-parts were produced on a DSM Xplore injection molding machine. The schematic of HA micro-sized component is depicted in Figure 2.

Solvent debinding was accomplished using an MMM VentiCell 111 oven. The palm stearin binder was taken out of the HA green micro-parts by immersing them in acetone for 50 min at 60 °C.

RESULTS AND DISCUSSION

The μ PIM process begins with mixing of powder and binder. The temperature and duration of the mixing process, the amount of powder added, the size of the powder, the sequence in which the ingredients are added, and the shear rate are all factors that affect the quality of the feedstock (Supati et al. 2000). Usually, the later phases of the process are unable to compensate for any flaws in the quality of the feedstock. An effective dispersion of the HA powder particles within the palm stearin and LDPE binders was achieved in this study with the use of a twin-screw-blade mixer during the mixing procedure. Figure 3 depicts the mixing curve of HA feedstock with powder loading of 57 vol.%. In this context, it is pertinent to mention that Salleh et al. (2017) prepared HA feedstocks with a range of powder loadings between 54 and 56 vol.% during their PIM experiment. The use of a mixer that correlated the measurement of the mixing torque with time allowed for the evaluation of the homogeneity of the HA feedstock. Based on Figure 3, the homogeneity of the feedstock was established by the steady value that was reached following an initial increase in the mixing torque throughout time. The existence of agglomerated clusters in the HA powder particles may have contributed to the initial rise in torque (Basir et al. 2021a). The preparation of homogeneous feedstock is favored in any μ PIM process. In addition to increasing the likelihood that a component may develop faults, inhomogeneous feedstock also has a detrimental impact on the mechanical properties of the component (Supati et al. 2000; Basir et al. 2021a). The FESEM image of the fabricated HA feedstock is displayed in Figure 4. Based on Figure 4, HA powder particles were adequately coated with binders.

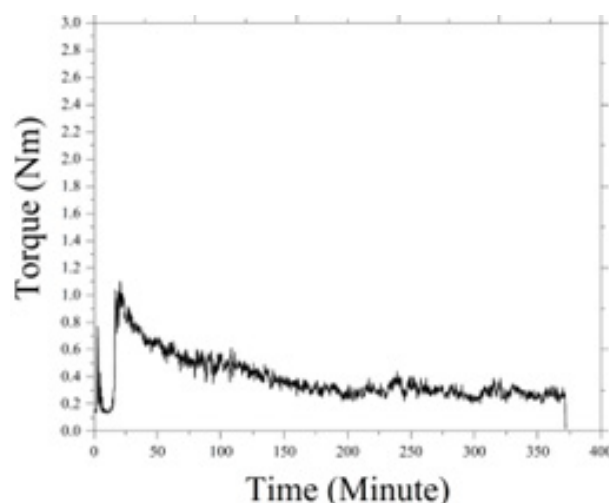


FIGURE 3. Mixing curve of HA feedstock

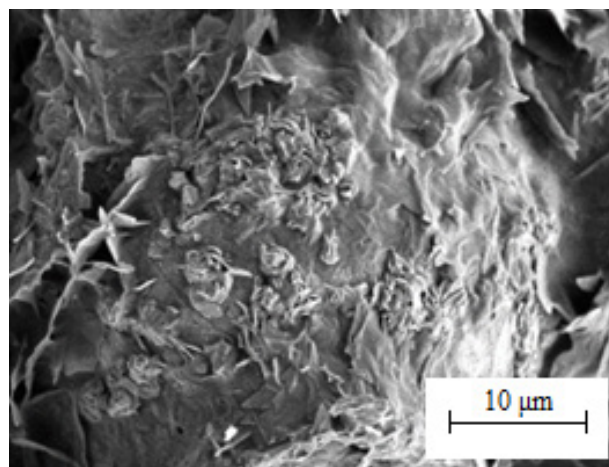


FIGURE 4. FESEM image of HA feedstock

In order to determine the proper injection molding parameters, micro-injection molding trials using HA feedstock were conducted. The injection molding settings utilized for producing HA micro-parts with no defects are displayed in Table 1. Micro-samples frequently had short shot defects when mold temperatures less than 110 °C were employed. An injection pressure higher than 12 bar was not employed during this study to prevent flash defects in the samples. Figure 5 depicts the green HA micro-part produced based on μ PIM technique. The FESEM image of the fabricated HA micro-specimen is shown in Figure 6. As can be seen in Figure 6, with addition to the HA powder particles being completely covered with binders, the micro-sample showed no signs of flaws or cracks.

TABLE 1. Injection parameters for HA micro-parts

Injection parameters	Operational process
Injection pressure	12 bar
Mold temperature	110 °C
Melt temperature	180 °C
Injection time	5 s

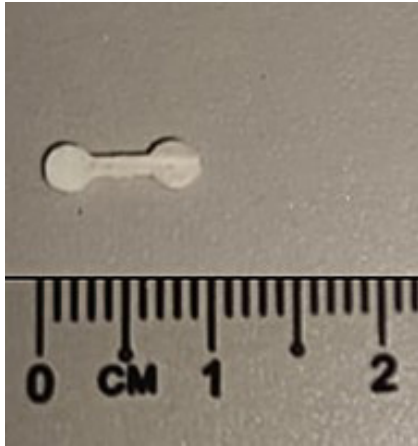


FIGURE 5. Photograph of green HA micro-part

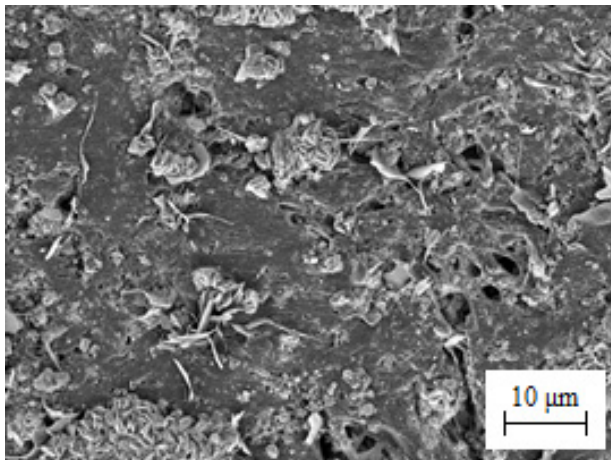


FIGURE 6. FESEM image of green HA micro-sized specimen

The solvent debinding procedure was carried out immediately following the injection molding procedure. The soluble binder is typically taken out of the green components during the solvent debinding procedure. There is a higher likelihood that defects and cracks will emerge in components during solvent debinding as components become fragile at this phase. According to Basir et al. (2021), the range of 30 to 60 °C was the most often employed temperature for solvent debinding by earlier PIM and μ PIM researchers. Based on this, solvent debinding was performed at 60 °C in the current study. Figure 7 depicts the extraction of palm stearin binder for the HA

micro-part with time. Based on Figure 7, during the first 20 minutes, the soluble binder was eliminated at a rather rapid pace; the next 30 minutes demonstrated a slowdown in that rate. After 50 min, 82.2% of the palm stearin was eliminated from the specimen. The image of the solvent debound HA micro-part is shown in Figure 8. Compared to the green part, no dimensional change was observed in the solvent debound part. The FESEM image of the solvent debound sample is illustrated in Figure 9. Based on Figure 9, in addition to a reasonable amount of palm stearin being removed, the specimen developed open pores, which were necessary to remove the insoluble LDPE binder during the thermal debinding phase. The thermal debinding and sintering processes of the HA micro-sized components processed through μ PIM will be discussed in our future study.

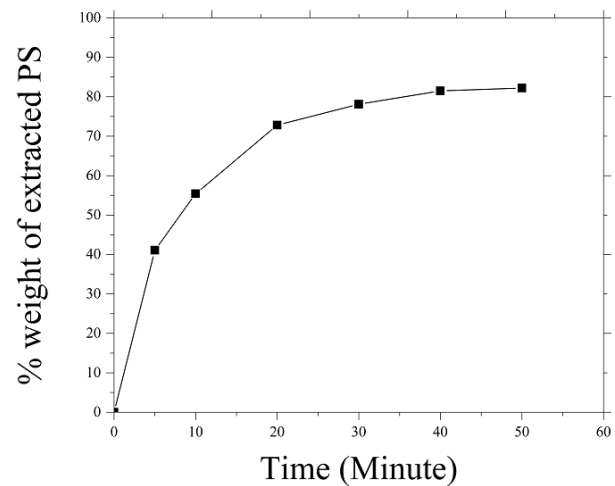


FIGURE 7. Palm stearin loss at 60 °C during solvent extraction

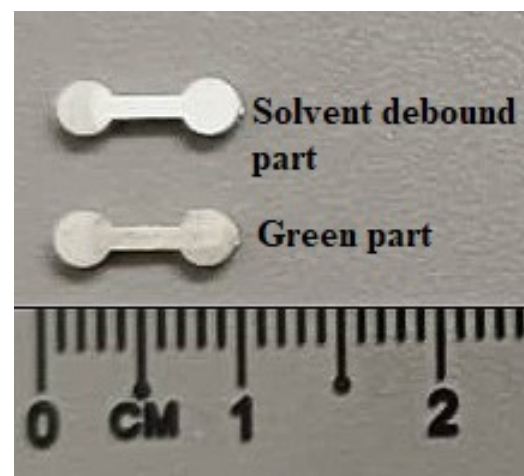


FIGURE 8. Comparison between green and solvent debound HA micro-part

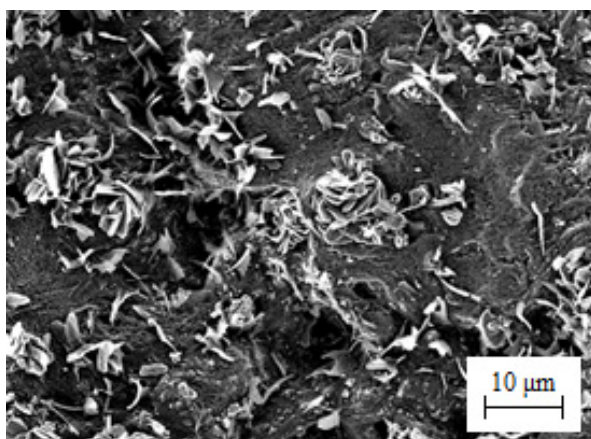


FIGURE 9. FESEM image of solvent debound HA micro-part

CONCLUSION

The aim of this study was to examine the moldability and solvent extraction behavior of μ PIM-processed HA micro-sized components. Homogeneous HA feedstock with a powder loading of 57 vol.% was produced by mixing powder and binders at 150 °C. Defect-free green HA micro-sized components were successfully fabricated by appropriately employing the injection molding parameters. At a temperature of 60 °C, solvent debinding was performed with 82.2% of the palm stearin binder effectively removed from the green part. The emergence of open pores in the solvent debound HA component will aid in the removal of the LDPE binder during the thermal extraction procedure. This study will contribute to a better understanding of the injection molding and solvent debinding of HA micro-parts.

ACKNOWLEDGEMENT

The authors would like to thank Universiti Kebangsaan Malaysia for the financial support under the grant DIP-2022-015.

DECLARATION OF COMPETING INTEREST

None

REFERENCES

- Aslam, M., Ahmad, F., Yusoff, P. S. M. B. M., Altaf, K. Omar, M. A. & German, R. M. 2016. Powder injection molding of biocompatible stainless steel biodevices. *Powder Technology* 295: 84–95.
- Attia, U. M., Hauata, M., Walton, I., Annicchiarico, D. & Alcock, J. R. 2014. Creating movable interfaces by micro-powder injection moulding. *Journal of Materials Processing Technology* 214 (2): 295–303.
- Attia, U. M. & Alcock, J. R. 2012. Fabrication of hollow, 3D, micro-scale metallic structures by micro-powder injection moulding. *Journal of Materials Processing Technology* 212 (10): 2148–2153.
- Aziz, S. N. A., Bakar, M. A. A. & Ismail, M. H. 2015. Effect of single based binder palm stearin on sintered properties of hydroxyapatite scaffold. *Applied Mechanics and Materials* 763: 36–40.
- Arifin, A., Sulong, A. B., Muhamad, N., Syarif, J. & Ramli, M. I. 2014. Material processing of hydroxyapatite and titanium alloy (HA/Ti) composite as implant materials using powder metallurgy: A review. *Materials & Design* 55: 165–175.
- Alshammari, M. H., Alshammari, A. O., Elabbasy, M. T., Zreiq, R., El-Morsy, M. A., Menazea, A. A. & El-Kader, M. F. H. A. 2023. Physicochemical characterization tungsten oxide modified hydroxyapatite embedded into polylactic acid nanocomposite for biomedical applications. *Results in Physics* 49: 106446.
- Basir, A., Muhamad, N., Sulong, A. B., Jamadon, N. H. & Foudzi, F. M. 2023. Recent Advances in Processing of Titanium and Titanium Alloys through Metal Injection Molding for Biomedical Applications: 2013–2022. *Materials* 16 (11): 3991.
- Basir, A., Sulong, A. B., Jamadon, N. H. & Muhamad, N. 2021a. Feedstock properties and debinding mechanism of yttria-stabilized zirconia/ stainless steel 17-4PH micro-components fabricated via two-component micro-powder injection molding process. *Ceramics International* 47 (14): 20476–20485.
- Basir, A., Sulong, A. B., Jamadon, N. H., Muhamad, N. & Emeka U. B. 2021b. Process parameters used in macro/micro powder injection molding: An overview. *Metals and Materials International* 27: 2023–2045.
- Basir, A., Sulong, A. B., Jamadon, N. H. & Muhamad, N. 2022a. Physical Properties of Sintered Stainless Steel 17-4PH Micro-Part Processed by Micro Powder Injection Molding. *Jurnal Kejuruteraan* 34(6): 1209–1214.

- Basir, A., Sulong, A. B., Jamadon, N. H. & Muhamad, N. 2022b. Sintering behavior of bi-material micro-component of 17-4PH stainless steel and yttria-stabilized zirconia produced by two-component micro-powder injection molding process. *Materials* 15 (6): 2059.
- Bitar, M., Friederici, V., Imgrund, P., Brose, C. & Bruinink, A. 2012. In vitro bioactivity of micro metal injection moulded stainless steel with defined surface features. *European Cells and Materials* 23: 333–347.
- Crozier-Bioud, T., Momeni, V., Gonzalez-Gutierrez, J., Kukla, C., Luca, S. & Rolere, S. 2023. Current challenges in NdFeB permanent magnets manufacturing by powder injection molding (PIM): A review. *Materials Today Physics* 34: 101082.
- Dehghan-Manshadi, A., StJohn, D., Dargusch, M., Chen, Y., Sun, J. F. & Qian, M. 2018. Metal injection moulding of non-spherical titanium powders: Processing, microstructure and mechanical properties. *Journal of Manufacturing Processes* 31: 416–423.
- Fayyaz, A., Muhamad, N., Sulong, A. B., Rajabi, J. & Wong, Y. N. 2014. Fabrication of cemented tungsten carbide components by micro-powder injection moulding. *Journal of Materials Processing Technology* 214(7): 1436–1444.
- Foudzi, F. M., Muhamad, N., Bakar Sulong, A. & Zakaria, H. 2013. Yttria stabilized zirconia formed by micro ceramic injection molding: Rheological properties and debinding effects on the sintered part. *Ceramics International* 39(3): 2665–2674.
- Fu, G., Loh, N. H., Tor, S. B., Murakoshi, Y. & Maeda, R. 2004. Replication of metal microstructures by micro powder injection molding. *Materials & Design* 25(8): 729–733.
- Hussin, M. S. F., Abdullah, H. Z., Idris, M. I. & Wahap, M. A. A. 2022. Extraction of natural hydroxyapatite for biomedical applications-A review. *Heliyon* 8: e10356.
- Jung, I. D., Park, J. M., Kang, T. G., Kim, S. J. & Park, S. J. 2015. Magneto-rheological model for computational analysis of magnetic micro powder injection molding. *Computational Materials Science* 100: 39–44.
- Li, H. W., Zhao, Y. P., Chen, G. Q., Li, M. H., Fu, X. S. & Zhou, W. L. 2022. Synergy of low-and high-density polyethylene in a binder system for powder injection molding of SiC ceramics. *Ceramics International* 48(17): 25513–25520.
- Liu, Y., Pan, Y., Sun, J., Wu, X., Zhang, J., Fan, K. & Lu, X. 2023a. Metal injection molding of high-performance Ti composite using hydride-dehydride (HDH) powder. *Journal of Manufacturing Processes* 89(3): 328–337.
- Liu, C., Lu, H., Qin, M., Wu, H., Zhang, Z., He, Q., Wang, Y., Jia, B. & Qu, X. 2023b. Effect of powders on aluminum nitride components fabricated by PIM. *Powder Technology* 420: 118409.
- Liu, L., Gao, Y. Y., Qi, X. T. & Qi, M. X. 2018. Effects of wall slip on ZrO₂ rheological behavior in micro powder injection molding. *Ceramics International* 44(14): 16282–16294.
- Martínková, M., Hausnerová, B., Huba, J., Martínek, T., Káčřová, S., Kašpárková, V. & Humpolíček, P. 2022. Powder injection molded ceramic scaffolds: The role of pores size and surface functionalization on the cytocompatibility. *Materials & Design* 224: 111274.
- Meng, J., Loh, N. H., Fu, G., Tay, B. Y. & Tor, S. B. 2011. Micro powder injection moulding of alumina micro-channel part. *Journal of the European Ceramic Society* 31(6): 1049–1056.
- Meng, J., Loh, N. H., Fu, G., Tor, S. B. & Tay, B. Y. 2010. Replication and characterization of 316L stainless steel micro-mixer by micro powder injection molding. *Journal of Alloys and Compounds* 496(1–2): 293–299.
- Orlovskii, V. P., Komlev, V. S. & Barinov, S. M. 2002. Hydroxyapatite and hydroxyapatite-based ceramics. *Inorganic Materials* 38: 973–984.
- Piotter, V., Bauer, W., Knitter, R., Mueller, M., Mueller, T. & Plewa, K. 2011. Powder injection moulding of metallic and ceramic micro parts. *Microsystem Technologies* 17(2): 251–263.
- Park, J. M., Han, J. S., Gal, C. W., Oh, J. W., Kim, J. H., Kate, K. H., Atre, S. V., Kim, Y. & Park, S. J. 2018. Fabrication of micro-sized piezoelectric structure using powder injection molding with separated mold system. *Ceramics International* 44(11): 12709–12716.
- Shu, C., He, H., Fan, B.-w., Li, J.-h., Wang, T., Li, D.-y., Li, Y.-m. & He, H. 2022. Biocompatibility of vascular stents manufactured using metal injection molding in animal experiments. *Transactions of Nonferrous Metals Society of China* 32(2): 569–580.
- Siddiqui, H. A., Pickering, K. L. & Mucalo, M. R. 2018. A Review on the use of hydroxyapatite carbonaceous structure composites in bone replacement materials for strengthening purposes. *Materials* 11(10): 1813.
- Supati, R., Khor, K. A. & Tor, S. B. 2000. Mixing and characterization of feedstock for powder injection molding. *Materials Letters* 46(2–3): 109–114.
- Salleh, F. M., Sulong, A. B., Foudzi, F., Mohamed, I. F., Azman, N. E. & Mas'ood, N. N. 2017. Flow behaviour characterization of hydroxyapatite for powder injection moulding (PIM). *Journal of Mechanical Engineering* 3(1): 77–88.
- Tafti, A. A., Demers, V., Vachon, G. & Brailovski, V. 2023. Influence of powder size on the moldability

- and sintered properties of irregular iron-based feedstock used in low-pressure powder injection molding. *Powder Technology* 420: 118395.
- Tay, B. Y., Loh, N.H., Tor, S. B., Ng, F. L., Fu, G. & Lu, X. H. 2009. Characterisation of micro gears produced by micro powder injection moulding. *Powder Technology* 188(3): 179–182.
- Tan, L., Yu, X., Wan, P. & Yang, K. 2013. Biodegradable materials for bone repairs: A review. *Journal of Materials Science & Technology* 29(6): 503–513.
- Wang, C. R., Xiao, H., Shao, K. W., Lu, Z. & Zhang, K. F. 2014. Densification and mechanical properties of boron carbide with micro-hole array by micro-powder injection molding. *Ceramics International* 40(6): 7915–7921.
- Wang, C., Li, Z., Tian, W., Li, Y., Tang, L., Pang, Q. & Chen, M. 2022. Micro powder injection molding of boron carbide components with SiC-Al₂O₃-Y₂O₃ sintering additives. *Chinese Journal of Aeronautics* 35(5): 429–440.